

Chemical Alteration of Poly(tetrafluoroethylene) (TFE) Teflon Induced by Exposure to Hyperthermal Atomic Oxygen

Gar B. Hoflund* and Michael L. Everett

Department of Chemical Engineering, University of Florida, Gainesville, Florida 32611

Received: March 7, 2004; In Final Form: August 3, 2004

In this study, the erosion of poly(tetrafluoroethylene) TFE Teflon by hyperthermal atomic oxygen (AO) has been examined using X-ray photoelectron spectroscopy (XPS). The initial F/C atom ratio of 1.66 decreases to 1.15 after a 2 h exposure to a flux of 2×10^{15} atoms/cm² s AO with an average kinetic energy ~ 5 eV. The F/C atom ratio is further reduced to a value of 0.90 after a 25 h exposure. The high-resolution XPS C 1s data indicate that new chemical states of carbon form as the F is removed, and that the relative amounts of these states depend on the F content of the near-surface region. The states are most likely due to C bonded only to one F atom and C bonded only to other C atoms. Exposures of the AO-damaged surface to research-grade O₂ results in chemisorption of a very small amount of O (~ 0.8 at. %); this indicates that large quantities of reactive sites are not formed during the chemical erosion by AO. Further exposure to AO removes this chemisorbed oxygen. After exposing the AO-exposed surface to air for 90 min, O₂ is chemisorbed and the F/C atom ratio is reduced to 0.68. Another 46 h of AO exposure results in removal of this O and a further decrease in the F/C atom ratio to 0.58.

Introduction

Polymers are attractive and desirable materials for use in space applications because they are lightweight and typically much easier to process using techniques such as extrusion, casting, and injection molding at relatively low temperatures compared to metals and ceramics. They also tend to be more flexible and offer a wide variety of choices, from optically transparent to opaque, rubbery to stiff, and conducting to insulating. Fluoroethylenepropylene (FEP) Teflon¹ is one material that is widely used as a thermal blanket for spacecraft flying in low earth orbit (LEO).² Thermal control is provided by lining the FEP Teflon with aluminum or silver. FEP Teflon has a high thermal emittance, and this system reflects a large fraction of the incident solar energy.

However, over the last two decades it has been well established that polymers undergo severe degradation that results in reduced spacecraft lifetimes. These materials degrade because spacecraft surfaces are exposed to high fluxes of atomic oxygen (AO), bombardment by low- and high-energy charged particles, thermal cycling, and the full spectrum of solar radiation. AO is the main constituent of the atmosphere in LEO. It is formed by dissociation of O₂ by ultraviolet radiation from the sun, resulting in an AO concentration of approximately 10^8 atoms/cm³. The actual flux of $\sim 10^{14}$ atoms/cm² s impinging on a spacecraft is high due to orbiting speeds of approximately 8 km/s. At these relative speeds, thermal AO collides with a kinetic energy of ~ 4.5 eV. These highly energetic collisions not only result in surface chemical reactions but also lead to a pure physical sputtering of the surface atoms. Many studies have been conducted in an effort to determine the mechanism of this degradation primarily caused by surface reactions with AO.^{3–10} However, these studies have all been carried out after exposing these highly reactive surfaces to air prior to analysis, thus

introducing artifacts that do not represent the true space environment. Recent studies have shown that exposure to air chemically alters the reactive surfaces formed during AO exposure.^{11–14} It is, therefore, essential that analysis of polymers exposed to AO be carried out in vacuo to avoid artifacts induced by air exposure.

Several studies have been conducted on the deterioration of fluorinated polymers retrieved from spacecraft subjected to the LEO environment. The outer layer of FEP Teflon multilayer insulation on the Hubble space telescope (HST) was significantly cracked at the time of the second HST servicing mission, 6.8 years after it was launched into LEO.^{15,16} Comparatively minor embrittlement and cracking were also observed in the materials retrieved from solar-facing surfaces on the HST at the time of the first servicing mission (3.6 years of exposure to LEO). Furthermore, an increased deterioration of fluorinated polymers may result from a synergistic effect of VUV radiation and charged particles such as electrons and ions in the presence of AO.¹⁷ This point will be examined in future studies.

The goal of this study is to examine and attempt to understand the chemical alterations of a TFE Teflon surface when impacted by hyperthermal (~ 5 eV) AO. The source used is described below. It is the best source available for simulating LEO because it produces a very pure flux of hyperthermal AO with no O₂, O or O₂ ions, electrons, or strong UV components. The average energy and energy spread are similar to AO in LEO. There are two types of bonds in TFE Teflon: C–C bonds and C–F bonds with bond strengths of approximately 83 and 111 kcal/mol, respectively. Intuitively low-energy AO would not be expected to break these bonds, and this has been found experimentally.⁵ Gindulyte et al.¹⁸ have carried out a quantum mechanical study on the erosion of Teflon by AO. They conclude that AO in LEO possesses enough translational energy to erode Teflon by breaking C–C bonds. They did not consider breakage of C–F bonds based on electronegativity arguments.

* Corresponding author. Fax: (352) 392-9513. E-mail: garho@hotmail.com.

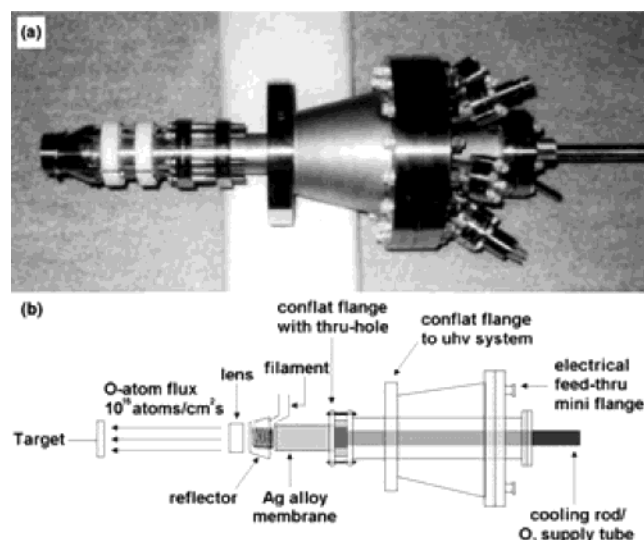


Figure 1. (a) Photograph of the atomic oxygen source and (b) schematic of the atomic oxygen source.

Experimental Section

O Atom Source Characteristics. A photograph and schematic diagram illustrating the operational principles of the electron-stimulated desorption (ESD), AO source are shown in Figure 1a and 1b, respectively. Ultrahigh purity O₂ dissociatively adsorbs on the high-pressure (2 Torr) side of a thin metallic Ag alloy membrane maintained at elevated temperature (~400 °C) and permeates through the membrane to the UHV side. There the chemisorbed atoms are struck by a directed flux of primary electrons, which results in ESD of O atoms forming a continuous flux. The primary electrons are produced by thermionic emission from a coiled hot filament supported around the perimeter of the membrane. An electron reflector (lens assembly) surrounds the filament. It produces a potential field, which creates a uniform flux of electrons over the membrane surface. These primary electrons have a kinetic energy of 1000 eV and provide two functions: ESD of the O atoms and heating of the membrane surface. Another lens is placed between the reflector and the sample for removal of all charged particles, including secondary electrons, O⁺, and O⁻ produced during the ESD process.

Several processes have to function in series at sufficiently high rates for this system to work, including dissociative chemisorption of O₂ on the metal surface, permeation of atomic oxygen through the membrane, and formation of the AO flux by ESD. Since these processes occur in series, the slowest one determines the magnitude of the AO flux. The sticking coefficient of O₂ on polycrystalline Ag (step 1) is fairly small (<0.001), so it is necessary to use a relatively high pressure on the upstream side of the membrane. However, the permeation rate through the membrane is proportional to the reciprocal of the membrane thickness. This means that it is desirable to have a high pressure and a thin membrane, but this can lead to membrane failure. The ESD rate can be increased by increasing the primary electron current to the membrane, but this increases the temperature of the membrane and can result in evaporation of Ag, which is unacceptable.

The AO produced by this source has been shown to be hyperthermal (energies greater than 0.01–0.02 eV), but the neutral energy distribution has not been measured. Corallo et al.¹⁹ have measured the energy distribution of O⁺ emitted by ESD from a Ag(110) surface and found that this distribution has a maximum of ~5 eV and a full-width at half-maximum of

3.6 eV. This ion energy distribution sets an upper bound for the neutral energy distribution because ESD neutrals are generally believed to be less energetic than ESD ions based on models of the ESD process. This point has been discussed often in the ESD literature but not actually demonstrated. Since neutral ESD species are difficult to detect, very few ESD studies of neutral species have appeared in the literature. The neutral-atom flux has been detected using a quadrupole mass spectrometer^{20,21} in the appearance potential (AP) mode to allow the atoms to be distinguished from residual gases and background gas products formed by collisions of the neutrals with the walls of the UHV system. In this experiment, the ion acceleration potential was set at 0.0 V. Calibration studies have demonstrated that the ions entering the quadrupole section must have a minimum kinetic energy of 2.0 eV to reach the detector, so the ESD neutrals detected have a minimum energy of 2.0 eV. Therefore, the hyperthermal AO produced by this ESD source have energies greater than 2 eV but possibly less than the ion energy distribution. Furthermore, these mass-spectrometric experiments have shown that the AO-to-O⁺ ratio is about 10⁸ and that the O⁺-to-O⁻ ratio is about 100.

Several approaches have been used to measure the magnitude of the hyperthermal AO flux and reasonable agreement was obtained between the various methods. The flux from the ESD-AO source is approximately 2×10^{15} atoms/cm² s. One of the most reliable methods for flux determination is the measurement of a ZrO₂ film growth rate.²² A Zr flux was generated by e⁻-beam evaporation and the flux was calibrated using a quartz-crystal monitor. Based on the facts that stoichiometric ZrO₂ was produced and that no O₂ is present in the AO flux, the AO flux was calculated. By doubling the Zr flux, stoichiometric ZrO was grown.²³ The AO flux has also been determined by measuring the chemisorption rate of AO on polycrystalline Au using ion scattering spectroscopy.²⁴ The flux determined using this method is in excellent agreement with that determined using the oxide growth rate method.

Surface Characterization. An as-received E. I. du Pont Nemours & Co., Inc. TFE Teflon film¹ was wiped with 2-propanol and inserted into the UHV chamber (base pressure < 1.0×10^{-10} Torr). The XPS measurements were performed using a double-pass, cylindrical-mirror analyzer (DPCMA) (PHI Model 25-270AR). The XPS survey spectra were taken in the retarding mode with a pass energy of 50 eV, and high-resolution XPS spectra were taken with a pass energy of 25 eV using Mg K α X-rays (PHI Model 04-151 X-ray source). Data collection was accomplished using a computer interfaced, digital-pulse-counting circuit²⁵ followed by smoothing with digital-filtering techniques.²⁶ The sample was tilted 30° off the axis of the DPCMA, and the DPCMA accepted electrons emitted into a cone 42.6 ± 6 degrees off the DPCMA axis.

The XPS spectra were first obtained from the as-entered, solvent-cleaned sample. The sample was then transferred into an adjoining UHV chamber that houses the ESD-AO source via a magnetically coupled rotary/linear manipulator. There the surface was exposed to a hyperthermal AO flux and reexamined after various exposure times. This chamber contains a 120 L/s ion pump that produces a base pressure in the low 10⁻⁹ Torr range during operation of the AO source. This chamber is very clean because the AO reacts with any contamination to form products that are pumped away. Many experiments have been performed, including the oxidation of a cleaned Si(111) surface by AO that demonstrates that hydrocarbon contamination does not accumulate at surfaces in this chamber. The sample was not exposed to air after the AO exposures and before collecting

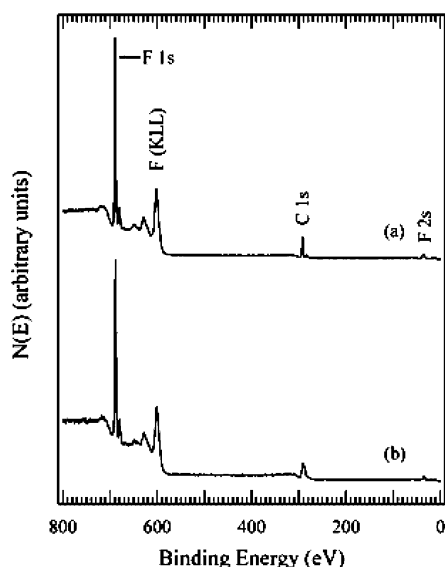


Figure 2. XPS survey spectra obtained from TFE Teflon (a) as entered and (b) after a 2 h exposure to AO.

XPS data. However, after the AO exposures the surfaces were exposed to O₂ and then air to determine how this would affect the AO-exposed surfaces. The approximate normal distance between the sample face and source in this study was 15 cm, at which distance the flux was $\sim 2.0 \times 10^{15}$ atoms/cm² s for the instrument settings used. The sample was maintained at room temperature during the AO exposures, with a temperature increase to about 50 °C during exposure to the X-ray source during XPS data collection. The substrate temperature was determined using a chromel–alumel thermocouple. The analysis chamber was pumped by a 400 L/s ion pump, a 180 L/s turbomolecular pump, and a 4000 L/s cryopump containing a Ti sublimation system. The pressure was $\sim 2 \times 10^{-10}$ Torr during collection of the XPS data. Under these conditions carbon contamination was not a problem. The X-ray source was a flood source, and the DPCMA accepted photoelectrons from a spot 4 mm in diameter. Charging did not present a difficulty in this study. The spectrum taken from TFE Teflon was shifted so that the C 1s and F 1s peaks were at the same binding energies (BEs) of reference spectra.²⁷ All other spectra were shifted by this same value. The specific treatments used were (1) exposure to AO for 2 h, (2) exposure to AO for a total of 24 h, (3) exposure to research-grade O₂ at room temperature and 150 Torr for 20 min, (4) exposure to AO for a total of 25 h, (5) exposure to AO for a total of 28 h, (6) exposure to air for 90 min at room temperature, and (7) exposure to AO for a total of 78 h. XPS spectra were collected after each treatment.

Results and Discussion

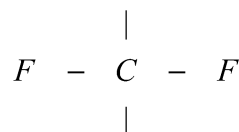
XPS survey spectra obtained from the TFE Teflon film before and after a 2 h exposure are shown in Figure 2a and b, respectively. Spectrum a is identical to that shown in the polymer XPS handbook by Beamson and Briggs²⁷ in that the C 1s, F 1s, F Auger (KLL), and F 2s peaks are present. An O 1s peak, which would appear near a BE of 530 eV, is not present. Estimates of the near-surface compositions have been made from the peak areas in the high-resolution spectra using published atomic-sensitivity factors²⁸ with the assumption of a homogeneous surface region. The near-surface region of the sample is probed with XPS and yields a weighted-average composition, with the atomic layers near the surface being weighted more heavily since the photoemitted electrons from these layers have

TABLE 1: Near-Surface Compositions of TFE Teflon after Various Treatments (At. %)

	F	O	C	F/C atom ratio	O/C atom ratio
as entered	62.4	0.0	37.6	1.66	0.0
AO 2 h	53.6	0.0	46.4	1.15	0.0
AO 24 h	47.4	0.0	52.6	0.90	0.0
O ₂ 20 min	46.8	0.8	52.4	0.90	0.015
AO 25 h	44.9	0.1	55.0	0.81	0.002
AO 28 h	45.2	0.0	54.8	0.82	0.0
air 90 min	39.8	1.9	58.3	0.68	0.03
AO 74 h	36.6	0.0	63.4	0.58	0.0

a lower probability of scattering inelastically. The sampling depth is ~ 4 – 6 nm, and $\sim 10\%$ of the signal originates from the outermost atomic layer.²⁹ This near-surface region is nonhomogeneous because the AO reacts most strongly with the outermost few atomic layers. Therefore, the region that reacts to the greatest extent with AO also makes the largest contribution to the XPS signal. This fact implies that XPS is an excellent technique for studying AO erosion of spacecraft materials. Even though the distribution functions involving the depth of chemical reactions in the near-surface region and the XPS determination of the weighted average composition of the near-surface region are complex, the compositional values provide a trend that is indicative of the chemical alterations occurring during AO exposure. The compositions determined using the homogeneous assumption are shown in Table 1 before and after various exposures to AO, O₂, and air. The F/C atom ratio obtained from the as-entered sample is 1.66, which is lower than the stoichiometric value of 2.0. This is most likely due to inaccuracies in the sensitivity factors used. The presence of adventitious carbon would result in a decreased F/C atom ratio. However, as discussed below with regard to the high-resolution C 1s spectra, only a small amount of adventitious carbon is present after the 2-propanol wipe. This carbon is removed rapidly by exposure to AO, so a destructive technique such as ion sputtering was not used to remove the adventitious carbon because this may create a damaged surface structure, which may react differently with AO. After a 2 h AO exposure (survey spectrum shown in Figure 2b), the F/C atom ratio is decreased from 1.66 to 1.15. That is, over 30% of the F is removed from the near-surface region by this short exposure.

The F features do not appear to change shapes or positions in the survey spectra obtained before and after the 2 h AO exposure. However, the shape of the C 1s peak is significantly altered. This is more apparent in the high-resolution spectra shown in Figure 3. The C 1s and F 1s features obtained from the as-entered TFE Teflon are shown in Figures 3Aa and 3Ca, respectively, and in Figures 3Ab and 3Cb for the surface exposed to AO for 2 h. The C 1s feature obtained from the as-entered TFE Teflon consists of a narrow, predominant peak with a BE of 292.5 eV and small features between 284 and 286 eV, which are due to hydrocarbon and possibly alcohol contamination. These features are removed by AO exposure. The C 1s feature obtained after the 2 h AO exposure is quite broad and complex. It consists of contributions from at least three different species with BEs of 292.5, 290.0, and 288.0 eV. Assigning the peaks to specific species is quite difficult for several reasons. Defining localized species that yield features at specific BEs may not be possible. For example,



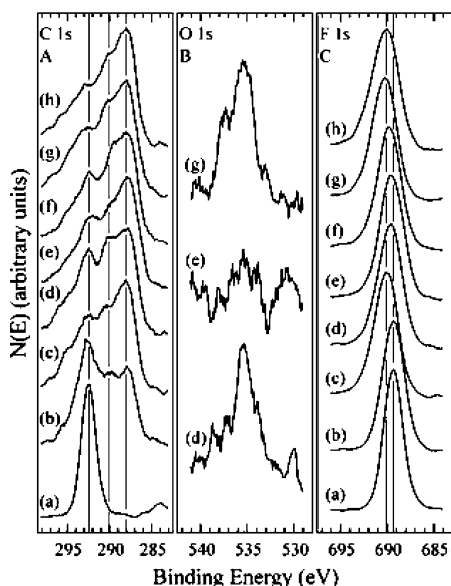
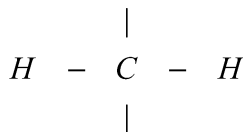


Figure 3. High-resolution XPS (A) C 1s, (B) O 1s, and (C) F 1s obtained from TFE Teflon (a) as entered, (b) after exposure to AO for 2 h, (c) after exposure to AO for a total of 24 h, (d) after exposure to research-grade O₂ at room temperature and 150 Torr for 20 min, (e) after exposure to AO for a total of 25 h, (f) after exposure to AO for a total of 28 h, (g) after exposure to air for 90 min at room temperature, and (h) after exposure to AO for a total of 74 h.

species are present in both TFE Teflon and Tefzel¹ (ethylene tetrafluoroethylene-ETFE), but the C 1s BEs are 292.48 and 290.9 eV, respectively. Also,



species are present in Tefzel and Tedlar¹ (vinyl fluoride-PVF) with BEs of 286.44 and 285.74 eV, respectively. The XPS BEs result from the chemical environment around the given element. This fact implies that the chemical environment is larger than the species defined in TFE Teflon, Tefzel, and Tedlar. Since there are distinct peaks in these spectra, there are distinct chemical environments, but defining the nature of this chemical environment is not possible. Furthermore, the hyperthermal AO-exposed surface is a damaged surface in that the composition is altered to a great extent and the structure is most likely altered as discussed below. The new features that appear in the C 1s spectrum after the 2 h AO exposure have lower BEs, indicating that the chemical environments responsible for these features are F depleted. This assertion is consistent with the compositional data shown in Table 1. However, there is a small shoulder on the high-BE side of the C 1s feature, which is believed to be due to emission from C species, which have lost valence electrons through emission of negative species during exposure to AO. The BE of the F 1s peak (Figure 3Cb) remains unchanged, but the peak is slightly broadened to the high-BE side. This indicates that the F remaining in the near-surface region more strongly attracts electrons.

An XPS survey spectrum obtained from the TFE Teflon surface after a 24 h AO exposure is shown in Figure 4a. The increased AO exposure results in a decrease in the F/C atom ratio from 1.15 to 0.90 (Table 1), and the C 1s peak shape is changed significantly from that after the 2 h AO exposure (Figure 2b). This is more apparent in the C 1s spectrum shown

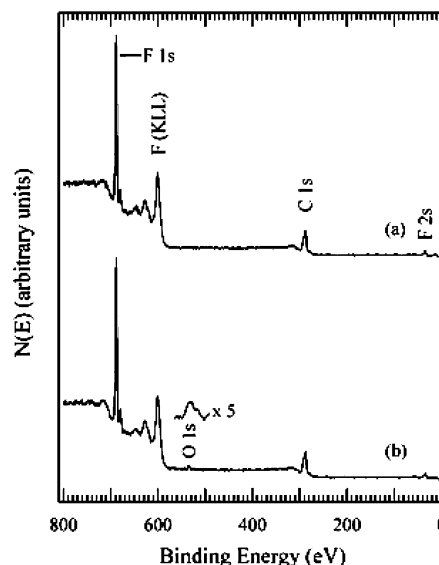


Figure 4. XPS survey spectra obtained from TFE Teflon (a) after a 24 h exposure to AO and (b) after a 20 min exposure to O₂ at room temperature and 150 Torr.

in Figure 3Ac. The feature with a BE of 288.0 eV is now most prominent and the feature due to TFE Teflon at a BE of 292.5 eV is the least prominent. These results demonstrate that hyperthermal AO exposure destroys the TFE Teflon structure by removing F from the near-surface region. The two states at BEs of 288.0 and 290.0 eV are due to F-depleted regions. The presence of lower concentrations of F implies that electron density on the C atoms is not decreased to such a large extent, resulting in increased C 1s BEs. The feature at 288.0 eV may be due to regions where all of the F has been removed. Also, the shoulder on the high-BE side of the C 1s feature is increased significantly in magnitude as expected, since it is the result of AO exposure. The corresponding F 1s feature is shown in Figure 3Cc. This feature is shifted from 689.3 to 690.0 eV. The increased BE indicates that the remaining F is able to attract and bind electrons more strongly from the damaged matrix as the F concentration is decreased.

Next, the 24 h, AO-exposed TFE Teflon surface was exposed to research-grade O₂ for 20 min at room temperature and 150 Torr. The XPS survey spectrum obtained from this surface is shown in Figure 4b. There appear to be negligible differences in the sizes and shapes of the C and F features before and after the O₂ exposure in these survey spectra, but a small peak due to O is apparent at a BE of 535.4 eV. This assignment is discussed further below. The fact that this surface dissociatively chemisorbs molecular oxygen implies that reactive sites are present on the AO-exposed TFE Teflon surface. The amount of O₂ that chemisorbs provides a measure of the concentration of reactive sites in the near-surface region. Previous studies have shown that AO-exposed Kapton,^{1,11} Tedlar,³⁰ and Tefzel³¹ chemisorb large amounts of molecular oxygen during a similar exposure to research-grade O₂. This indicates that these surfaces contain a high concentration of reactive sites. These reactive sites are probably present because cross bonding cannot occur due to geometrical constraints. These polymers all contain H that may react with AO to form water, which desorbs. The amount of molecular oxygen chemisorbed on AO-exposed TFE Teflon is very small, indicating that the concentration of reactive species is quite small. The data in Table 1 indicate that much of the F initially present is removed by the AO exposure. Since very little O₂ chemisorbs, the broken bonds formed by AO

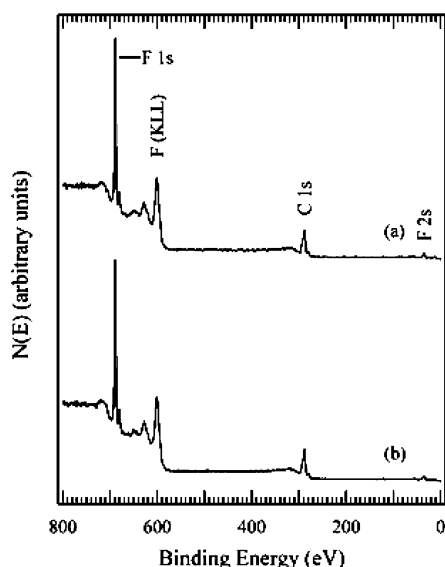


Figure 5. XPS survey spectra obtained from TFE Teflon (a) after a 25 h exposure to AO (1 h AO exposure after the O₂ exposure) and (b) after 28 h total AO exposure.

exposure must crosslink in TFE Teflon. Teflon does not contain H, so formation of water is not possible in this case.

Although the peak shapes are similar before and after the research-grade O₂ exposure in the survey spectra, quite significant differences are apparent in the high-resolution spectra (Figures 3Ad and 3Cd). Specifically, the feature due to F in TFE Teflon at 292.5 eV is increased in intensity relative to the F-depleted state at 288.0 eV. Since the AO reacts most strongly with TFE Teflon right at the surface, the AO-exposed surface is most likely a layered structure with the most F-depleted state at the surface (288.0 eV), the next most F-depleted state just beneath (290.0 eV), and the TFE Teflon structure (292.5 eV) beneath these two layers. A possibility is that the O₂ reacts with the F-depleted layer at the surface to form CO or CO₂. This removes part of the top layer, making the underlying two layers more prominent in the XPS spectra. This also explains why the oxygen content of the O₂-exposed surface is so low (<1 at. %). The outermost layer is a damaged layer with many vacancies and defects, which would make it quite reactive chemically. The very small high-resolution O 1s feature is shown in Figure 3Bd. It is narrow, indicating that one chemical state of oxygen is predominant. It is also broadened on the low-BE side, indicating the presence of a second oxygen chemical state. The fact that this peak is present demonstrates that the O₂ bond can be broken at the AO-exposed TFE Teflon surface under the O₂-exposure conditions used. The corresponding F 1s feature is shown in Figure 3Cd. It is shifted toward the BE of F in TFE Teflon and is broadened. This indicates that this feature is composed of contributions from F in the middle F-depleted layer and F in TFE Teflon.

The O₂-exposed surface was then exposed to AO for 1 h (total AO exposure of 25 h), and the resulting XPS survey spectrum is shown in Figure 5a. The O 1s peak is not present, indicating that AO removes chemisorbed O from the O₂-exposed, AO-exposed TFE Teflon surface. The compositional data in Table 1 indicate that the near-surface O concentration decreases from 0.8 to 0.1 at. % by the AO exposure. The mechanism of O removal may be physical sputtering or chemical reaction to form O₂ or CO₂. The F/C atom ratio is again decreased from 0.895 to 0.816. This is less than one-half of the F initially present. More information is provided by the high-resolution spectra shown in Figure 3. In the C 1s spectrum (Figure 3Ae), the

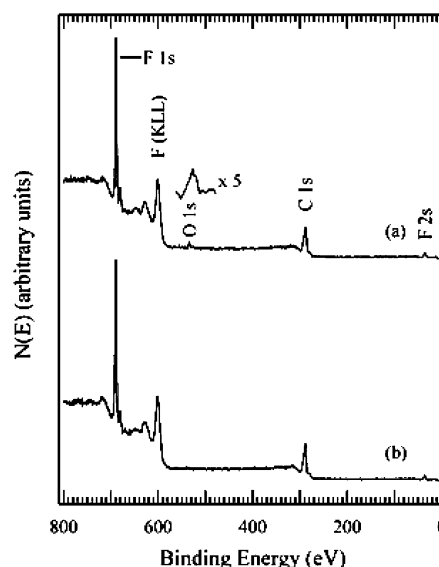


Figure 6. XPS survey spectra obtained from AO-exposed TFE Teflon (a) after a 90 min exposure to air at room temperature and (b) after a total of 74 h exposure to AO (46 h of AO exposure after the air exposure).

F-depleted near-surface region again yields the most prominent feature, as it did before the O₂ exposure (Figure 3Ac). The peak due to the TFE Teflon structure is reduced in magnitude, but not to that before the O₂ exposure. The O 1s feature shown in Figure 3Be is essentially at the noise level, indicating that the chemisorbed O is removed by the AO exposure. The F 1s feature (Figure 3Ce) is not changed significantly by the 1 h AO exposure, though it may have shifted slightly back toward higher BEs.

Another 3 h exposure to AO results only in small changes, which are not apparent in the survey spectrum shown in Figure 5b. According to the data in Table 1, the F/C atom ratio remains unchanged in the near-surface region but the last small amount of chemisorbed O is removed. Changes in the high-resolution C 1s and F 1s features shown in Figures 3Af and 3Cf, respectively, are also small. The F 1s peak is shifted a few tenths of an eV toward higher BEs, which is characteristic of larger AO exposures.

The surface was then exposed to air for 90 min at room temperature. This treatment is quite different from an exposure to research-grade O₂ because air contains water, hydrocarbons, alcohols, and CO₂, which may adsorb at a surface. The XPS survey spectra obtained after this treatment is shown in Figure 6a. A small O 1s peak is apparent that is larger than the O 1s peak obtained after the research-grade O₂ exposure (Figure 4b). This is consistent with the compositional data in Table 1 that gives an oxygen concentration of 1.9 at. %. The research-grade O₂ exposure does not alter the F/C atom ratio, while the air exposure lowers the F/C atom ratio from 0.82 to 0.68, due to both an increase in the C concentration and a decrease in the F concentration. The high-resolution C 1s, O 1s, and F 1s spectra obtained after the air exposure are shown in Figures 3Ag, 3Bg, and 3Cg, respectively. After the research-grade O₂ exposure, the C 1s feature at 288.0 eV due to C in the damaged layer is significantly decreased, while this feature is significantly enhanced after the air exposure. This is due to chemisorption of hydrocarbons, and possibly alcohols, from the air. Since hydrocarbons and alcohol C 1s features are not present in the 284–286 BE region, the airborne organic species must react with the damaged layer, thereby enhancing the thickness of this layer. This explains how the damaged layer is enhanced relative

TABLE 2: Near-Surface Compositions of Tefzel after Various Treatments (At. %)

	F	O	C	F/C atom ratio	O/C atom ratio
as entered	41.5	2.3	56.2	0.74	0.04
AO 2 h	14.5	0.7	84.8	0.17	0.01
AO 24 h	1.9	3.5	94.7	0.02	0.04
O ₂ 20 min	3.7	7.2	89.1	0.04	0.08
AO 25 h	1.7	6.8	91.5	0.02	0.07
AO 28 h	1.2	4.9	93.9	0.01	0.05

to the middle layer and underlying TFE Teflon. The thickened damaged layer results in an increase in the C 1s signal and a decrease in the F 1s signal because the F now lies further beneath the surface. This explains the significant decrease in the F/C atom ratio by air exposure. The shape of the O 1s feature in Figure 3Bg is quite different from that obtained after the research-grade O₂ exposure (Figure 3Ba) in that it contains a large shoulder at a BE about 2 eV higher than the predominant feature. If this contribution is subtracted from the O 1s feature, the magnitudes of the chemisorbed O are similar for the research-grade O₂ exposure and the air exposure. This shoulder may be due to a species such as $-\text{CF}_2-\text{O}-\text{CF}_2-$, which has a C 1s BE of ~ 536 eV.²⁷ This is unlikely since the outermost region is F depleted. Another more likely possibility is that this O is bonded to e⁻-depleted C. This C may attract electrons away from O, resulting in a large O 1s BE. A very small amount of this species may be present after the research-grade O₂ exposure (Figure 3Bd). The difference may be due to the carbonaceous layer formed by reaction with airborne organics, the fact that the air exposure yields an O₂ exposure that is ~ 4.5 times greater than the research-grade O₂ exposure, or a combination of both. The F 1s peak is shifted toward the BE characteristic of an AO-exposed surface. This is consistent with the assertion that the depth of the damaged layer is enhanced by the air exposure.

The final treatment was an exposure to the AO flux for another 46 h (74 h total). This exposure is long enough to represent a steady state in which the surface continually erodes away at a constant rate but no further changes are observed in the surface chemistry. The survey spectrum obtained after this AO exposure is shown in Figure 6b. The O 1s feature is not present, indicating that AO removes surface O as found after the research-grade O₂ exposure. The F/C atom ratio (Table 1) is decreased to a value of 0.58. The series of exposures used in this study results in removal of approximately two-thirds of the F in the near-surface region most likely by a physical-sputtering mechanism. This is the first step in the AO erosion of TFE Teflon. A F-depleted C layer is left at the surface that erodes more slowly. The corresponding high-resolution C 1s and F 1s spectra are shown in Figures 3Ah and 3Ch, respectively. These spectra are most similar to those obtained after the 24 h AO exposure. The outermost F-depleted C layer is predominant, and the top two F-depleted layers are so thick that the TFE Teflon peak at 292.5 eV is quite small. Based on mean-free-path arguments, the F-depleted layer is probably about 3 nm thick. The F 1s peak has a BE of 690.0 eV, which is characteristic of an AO-exposed TFE Teflon surface. Hence, the TFE Teflon structure makes only a small contribution to this surface.

Similar AO-exposure studies have been carried out on Tefzel and Tedlar, and the XPS compositional results corresponding to Table 1 for TFE Teflon are shown in Tables 2 and 3, respectively. The F content of the near-surface region decreases rapidly for Tedlar, less rapidly for Tefzel, and relatively slowly for TFE Teflon with increasing AO fluence. This behavior correlates with the hydrogen content of these polymers. Tedlar is 50 at. % H, Tefzel is 33 at. % H, and TFE Teflon is 0 at. %

TABLE 3: Near-Surface Compositions of Tedlar after Various Treatments (At. %)

	F	O	C	F/C atom ratio	O/C atom ratio
as entered	29.0	7.2	63.7	0.45	0.11
AO 2 h	1.7	4.0	94.2	0.018	0.04
AO 24 h	2.0	6.3	91.7	0.022	0.071
O ₂ 20 min	1.1	10.4	88.5	0.012	0.12
AO 25 h	1.3	7.0	91.7	0.014	0.08
AO 28 h	1.7	6.7	91.6	0.018	0.07

H. This information suggests that H atoms; that is, H–C bonds, provide an attack point for AO, possibly through formation of water. After the surface structure is damaged, the F is susceptible to removal by AO. Since TFE Teflon does not contain H, the F is more difficult to remove. Furthermore, the C removal rate by AO is not much slower than the F removal rate, so the F/C atom ratio only decreases from 1.66 to about 0.58 for the steady-state surface composition. This is quite different than Tedlar, where the F/C atom ratio drops from 0.45 to 0.01, and Tefzel, where the F/C atom ratio drops from 0.74 to 0.01. The steady-state compositions of AO-exposed Tedlar and Tefzel are nearly identical, containing 91.7 and 94.7 at. % C respectively, while that for TFE Teflon is very different and contains only 63.4 at. % C. The reactions of the steady-state, AO-eroded surfaces with O₂ are also quite different. The O contents of both Tedlar and Tefzel are significantly increased after the O₂ exposure (O/C atom ratios increase from 0.07 to 0.12 for Tedlar and from 0.04 to 0.08 for Tefzel), while that for TFE Teflon only increases from 0.0 to 0.015. Again, this behavior correlates with the initial H content of the polymer.

Summary

In this study, the chemical alterations at a TFE Teflon surface caused by exposure to hyperthermal (~ 5 eV) AO have been studied using XPS. A 2 h exposure to AO results in a decrease in the F/C atom ratio from 1.66 to 1.15 and the formation of two new carbon chemical states assigned as C bonded to only one F and C bonded to other C. Another 22 h of AO exposure results in a further decrease of the F/C atom ratio to 0.90 and an increase in the concentration of the two new carbon states, with the C-bonding-to-C state predominating. Exposure of this AO-exposed surface to research-grade O₂ results in a small amount (0.8 at. %) of chemisorbed O due to dissociative bonding at reactive sites. The fact that so little O₂ chemisorbs indicates that the surface carbon bonds to other carbon, which is consistent with the formation of the new C chemical states. The chemisorbed O may be present in three different chemical states. Further exposure of this surface to AO for 3 h results in removal of the chemisorbed oxygen and a further reduction in the F/C atom ratio to 0.82. Then, this AO-exposed surface was exposed to air. The O₂ is chemisorbed in small quantities (1.9 total O at. %). Another 46 h of AO exposure results in removal of the chemisorbed O and a further reduction in the F/C atom ratio to 0.58.

Similar AO exposures on both Tedlar and Tefzel result in nearly complete removal of the F. These AO-exposed surfaces also chemisorb larger amounts of O relative to AO-exposed TFE Teflon when exposed to O₂ or air. This indicates that reactive radicals remain at AO-exposed surfaces of Tedlar and Tefzel in relatively high concentrations compared to TFE Teflon. The difference between TFE Teflon and Tedlar and Tefzel is that TFE Teflon does not contain C–H bonds. These facts indicate that C–H bonds are particularly susceptible to attack by AO, most likely by forming water. Then, the F is susceptible to nearly

complete removal. This does not occur with TFE Teflon since it has no C–H bonds.

Acknowledgment. Support for this research was received from the AFOSR through Grant No. F49620-01-0338.

References and Notes

- (1) TFE Teflon, FEP Teflon, Tefzel, Tedlar, and Kapton are registered trademark names by E. I. du Pont Nemours & Co., Inc.
- (2) Banks, B. A. The Use of Fluoropolymers in Space Applications. In *Modern Fluoropolymers*; John Wiley & Sons: New York, 1997.
- (3) Leger, L. J.; Visentine, J. T. *J. Spacecraft Rockets* **1986**, 23, 505.
- (4) Koontz, S. L.; Leger, L. J.; Visentine, J. T.; Hunton, D. E.; Cross, J. B.; Hakes, C. L. *J. Spacecraft Rockets* **1995**, 32, 483.
- (5) Tennyson, R. C. *Can. J. Phys.* **1991**, 69, 1190.
- (6) Koontz, S. L.; Leger, L. J.; Rickman, S. L.; Hakes, C. L.; Bui, D. T.; Hunton, D. E.; Cross, J. B. *J. Spacecraft Rockets* **1995**, 32, 475.
- (7) Reddy, M. R. *J. Mater. Sci.* **1995**, 30, 281.
- (8) Packirisamy, S.; Schwam, D.; Litt, M. H. *J. Mater. Sci.* **1995**, 30, 308.
- (9) Reddy, M. R.; Srinivasamurthy, N.; Agrawal, B. L. *Eur. Space Agency J.* **1992**, 16, 193.
- (10) de Groh, K. K.; Banks, B. A. *J. Spacecraft Rockets* **1994**, 31, 656.
- (11) Grossman, E.; Lifshitz, Y.; Wolan, J. T.; Mount, C. K.; Hoflund, G. B. *J. Spacecraft Rockets* **1999**, 36, 75.
- (12) Gonzalez, R. I.; Phillips, S. H.; Hoflund, G. B. *J. Spacecraft Rockets* **2000**, 37, 463.
- (13) Phillips, S. H.; Hoflund, G. B.; Gonzalez, R. I. *Proc. 45th International SAMPE Symposium*; 2000; 45, 1921.
- (14) Hoflund, G. B.; Gonzalez, R. I.; Phillips, S. H. *J. Adhesion Sci. Technol.* **2001**, 15, 1199.
- (15) DeGroh, K. K.; Gaier, J. R.; Espe, M. P.; Cato, D. R.; Sutter, J. K.; Scheiman, D. A. *High Perform. Polym.* **2000**, 12, 83.
- (16) Dever, J. A.; DeGroh, K. K.; Banks, B. A.; Townsend, J. A.; Barth, J. L.; Thomson, S.; Gregory, T.; Savage, W. *High Perform. Polym.* **2000**, 12, 125.
- (17) Rasoul, F. A.; Hill, D. J. T.; Forsythe, J. S.; O'Donnell, J. H.; George, G. A.; Pomery, P. J.; Young, P. R.; Connell, J. W. *J. Appl. Polym. Sci.* **1995**, 58, 1857.
- (18) Gindulyte, A.; Massa, L.; Banks, B. A.; Miller, S. K. R. *J. Phys. Chem. A* **2002**, 106, 5463.
- (19) Corallo, G. R.; Hoflund, G. B.; Outlaw, R. A. *Surf. Interface Anal.* **1988**, 12, 185.
- (20) Davidson, M. R.; Hoflund, G. B.; Outlaw, R. A. *Surf. Sci.* **1993**, 281, 111.
- (21) Outlaw, R. A.; Hoflund, G. B.; Corallo, G. R. *Appl. Surf. Sci.* **1987**, 28, 235.
- (22) Wisotzki, E.; Balogh, A. G.; Horst, H.; Wolan, J. T.; Hoflund, G. B. *J. Vac. Sci. Technol., A* **1999**, 17, 14.
- (23) Wisotzki, E.; Hahn, H.; Hoflund, G. B. In *Trends and New Applications of Thin Films*; Horst Hoffman, Trans Tech Publications Ltd: Switzerland, 1998; 181, pp 277–278.
- (24) Davidson, M. R.; Hoflund, G. B.; Outlaw, R. A. *J. Vac. Sci. Technol., A* **1993**, 11, 264.
- (25) Gilbert, R. E.; Cox, D. F.; Hoflund, G. B. *Rev. Sci. Instrum.* **1982**, 53, 1281.
- (26) Savitzky, A.; Golay, M. J. E. *Anal. Chem.* **1964**, 36, 1627.
- (27) *High-Resolution XPS of Organic Polymers: The Scienta ESCA300 Database*; Beamson, G., Briggs, D., Eds.; Wiley: Chichester, 1992; pp 54, 226–236.
- (28) *Handbook of X-ray Photoelectron Spectroscopy*; Wagner, C. D., Riggs, W. M., Davis, L. E., Moulder, J. F., Muilenberg, G. E., Eds.; Perkin-Elmer Corp.: Eden Prairie, MN, 1979.
- (29) Hoflund, G. B. In *Handbook of Surface and Interface Analysis: Methods in Problem Solving*; Rivière, J. C., Myhra, S., Eds.; Marcel Dekker: New York, 1998; pp 57–158.
- (30) Hoflund, G. B.; Everett, M. L. *Appl. Surf. Sci.* **2004**.
- (31) Everett, M. L.; Hoflund, G. B. *Macromolecules* **2004**.